Http://www.geojournals.cn/dzxbcn/ch/index.aspx

Fluid Inclusions of Calcite and Sources of Ore-forming Fluids in the Huize Zn-Pb-(Ag-Ge) District, Yunnan, China

HAN Runsheng[1, 2], LIU Congqiang[3], HUANG Zhilong[1],
MA Deyun[1, 2], LI Yuan[2], HU Bin[2], MA Gengsheng[2] and LEI Li[2]

1 Open Laboratory of Ore Deposit Geochemistry, Institute of Geochemistry,
Chinese Academy of Sciences, Guiyang, Guizhou 550002; E-mail: hrs331@sohu.com
2 Kunming University of Science and Technology, Kunming, Yunnan 650093
3 Institute of Geochemistry, Chinese Academy of Sciences, Guiyang, Guizhou 550002

Abstract   The Huize Zn-Pb- (Ag-Ge) district is a typical representative of the well-known medium-to large-sized carbonate-hosted Zn-Pb- (Ag-Ge) deposits, occurring in the Sichuan-Yunnan-Guizhou Pb-Zn Ore-forming Zone. Generally, fluid inclusions within calcite, one of the major gangue minerals, are dominated by two kinds of small (1–10 µm) inclusions including pure-liquid and liquid. The inclusions exist in concentrated groups along the crystal planes of the calcite. The ore-forming fluids containing Pb and Zn, which belong to the Na^+-K^+-Ca^{2+}-Cl^--F^--SO_4^{2-} type, are characterized by temperatures of 164-221°C, medium salinity in 5-10.8 wt% NaCl, and medium pressure at 410×10^5 to 661×10^5 Pa. The contents of Na^+-K^+ and Cl^--F^-, and ratios of Na^+/K^+-Cl^-/F^- in fluid inclusions present good linearity. The ratios of Na^+/K^+ (4.66–6.71) and Cl^-/F^- (18.21–31.04) in the fluid inclusions of calcite are relatively high, while those of Na^+/K^+ (0.29–5.69) and Cl^-/F^- (5.00–26.0) in the inclusions of sphalerite and pyrite are relatively low. The ratio of Na^+/K^+ increases in accord with those of Cl^-/F^-, which indicates that ore-forming fluid of deep source participates in the mineralization. The waters of fluid inclusions have δD values from −43.5‰ to −55.4‰ of calcite. The $\delta^{18}O_{V-SMOW}$ values of the ore-forming fluids, calculated values, range from 17.09‰ to 18.56‰ of calcite and 17.80‰ to 23.14‰ for dolomite. $\delta^{13}C_{V-PDB}$ values range from −1.94‰ to −3.31‰ for calcite and −3.35‰ to 0.85‰ for the ore-bearing dolomite. These data better demonstrate that the ore-forming fluids were mainly derived from metamorphic water and magmatic hot fluid, in relation to the metamorphism of the Kunyang Group in the basement and magmatic hydrothermalism. The deposit itself might have resulted from ascending cycles of ore-forming fluid, enriched in Pb and Zn. The Huize Zn-Pb- (Ag-Ge) deposits related to carbonate-hosted Zn-Pb sulphides.

Key words: Fluid geochemistry, fluid inclusion, hydrogen, oxygen and carbon isotopes, Huize Zn-Pb-(Ag-Ge) district, Yunnan, China

1 Introduction

Fluid is the quintessence of ore-formation. Its source, migration and relaxation represent the whole process of mineralization (Mao et al., 1999). Its major function in the ore-forming process has been the focus of the research projects of deposit and geological workers (Fyfe et al., 1978; Meissner and Wever, 1992; Robert et al., 1995; Zhai, 1996; Lu, 1997, 1998; Jia, 1996; Li et al., 1996; Peng and Dai, 1999; Mao and Li, 2001). Ettner et al. (1993) and Parry (1998) studied the fluid composition in fault structures, fluid inclusion and isotope composition. Bierlein et al. (1996) and Polliand et al. (1999) studied the structure and genesis of fluid forming orebodies (veins). The Huize Zn-Pb- (Ag-Ge) district is typical of Zn-Pb- (Ag) deposits occurring in the Sichuan-Yunnan-Guizhou Pb-Zn Ore-forming Belt in China. Due to the ore-forming geological conditions in the region, large-sized rich Zn-Pb- (Ag-Ge) deposits with unique geological features are thus formed (Han et al., 2002). Previous research (Liao, 1984; Chen,

1984; Zhang, 1984; Chen, 1993; Zhao, 1995; Liu, 1996; Han et al., 2000, 2001a, b) focused mainly on the geology of the deposits. However, the composition and physical-chemical parameters of ore-forming fluids are still poorly understood.

The sources of ore-forming fluids are discussed in this paper based mainly on research into fluid inclusions, carbon, hydrogen, and oxygen isotope composition.

2 Geology of Deposits

The Huize Zn-Pb-(Ag-Ge) district is located in the sagged Yunnan basin at the southern end of the Yangtze Platform. It consists mainly of the large Kuangshanchang and Qilinchang Zn-Pb-(Ag-Ge) deposits and the northeastern end of the Yinchangpo Ag-Pb-Zn deposit (Fig. 1). It lies in a structurally compounding position, which is produced by a north-east-trending fault-fold belt, a south-north-trending fault-fold belt, and a northwest-trending fault-fold belt that are controlled by the Xiaojiang fault
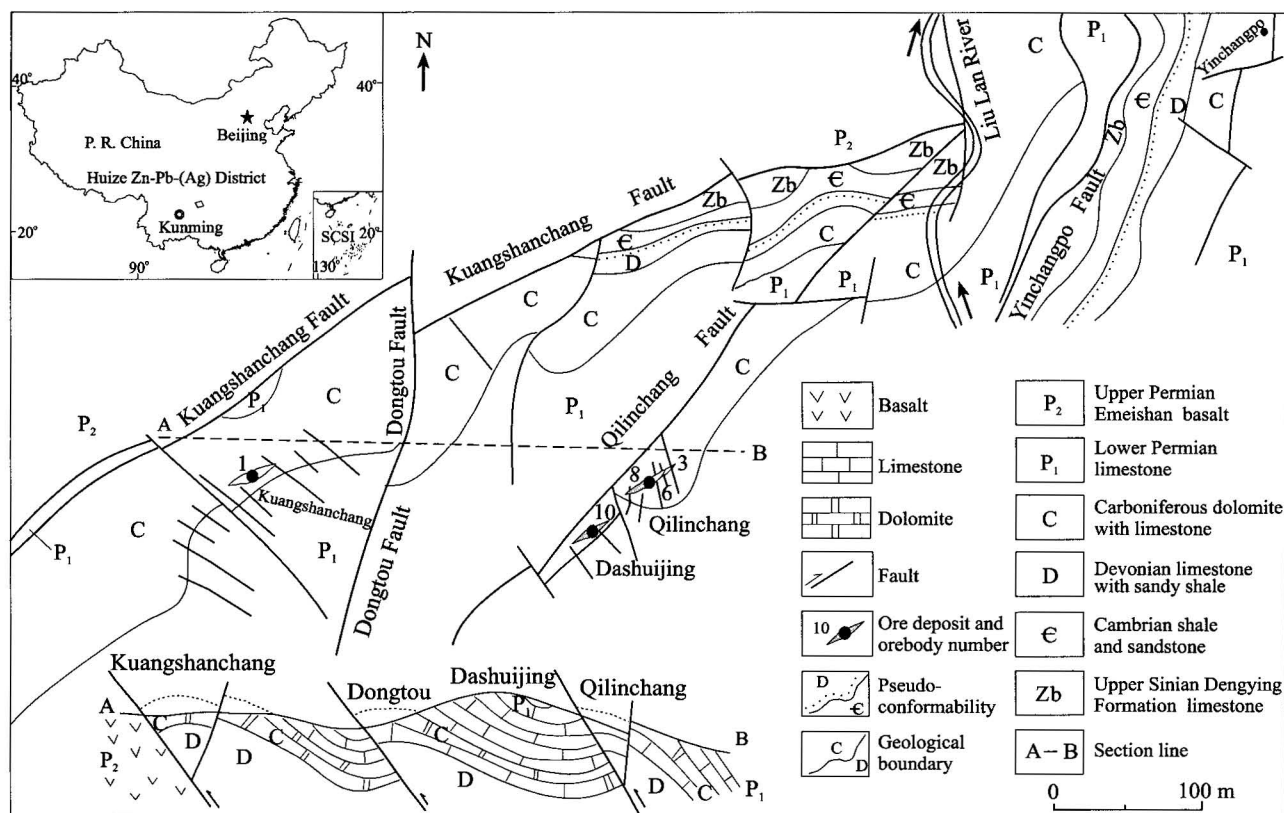
Fig. 1. Geological sketch map of the Huize Zn-Pb-(Ag-Ge) mining district.

zone and the concealed SN-trending Zhaotong-Qujing fault zone. The district has a two-strata structure, the basement being composed of the Proterozoic Kunyang base (unexposed), the Upper Sinian System and Paleozoic rocks. Predominant in the cover are the Upper Devonian, Carboniferous and Permian systems. Strata include the Upper Sinian Dengying Formation and the Lower Carboniferous Baizuo Formation. The latter formation is the most important ore-bearing stratum, which is mainly composed of grayish to white, pinkish, ream coarse-grained dolomite, and compact lumpy light yellow limestone and siliceous limestone. Faults are found in Kuangshanchang, Qilinchang and Yinchangpo, which are characterized by multiple period activities and a close relationship with mineralization. The juvenile motion is dominated by the Upper Permian Emeishan basalt eruption, which outcrops in the outer surrounds of the district.

There are about 30 Zn-Pb orebodies scattered throughout the district. With varying shapes such as vein, chamber, short column and stratiform, the orebodies are confined to a limited area in the fault zones of the mid- and Upper Baizuo Formation. The phenomena of taper-out, expansion and contraction are frequently observed. From the hanging-wall to the foot-wall rocks the main orebodies are an orderly arranged sub-zone phenomenon with the mineral assemblages of coarse grained pyrite-ferrous sphalerite→sphalerite–galena→fine-grained pyrite-carbonate. The ore grade of Pb and Zn is high up to 25%–35% principally with compact lump shape. Besides enriched Pb, Zn, Fe, S and Ag, there are other dispersed elements including Ge, In, Cd, Tl and Ga. Mineral composition in the ores mainly includes sphalerite, galena, pyrite, calcite and dolomite. Except for the fact that dolomitization is widely observed in wall-rock alteration, other alterations like silicification, pyritization and carbonatization are only scattered in a limited range of orebodies and near-surrounding rocks. Dolomite is a major ore-hosting wall rock that can be divided into two kinds of rock with sedimentary and hydrothermal alterations according to the formation: sedimentary dolomite is in laminated form with stable attitude; the relicts of altered dolomite and dolomitized limestone show an obvious gradual relationship. Frequently seen in the relicts are dolomite network and fine veins with unclear bedding. Dolomite crystals are coarse with crystal void highly developed in white, gray-white and pinkish colors.

The ore-forming process for the deposits includes a sedimentary diagenetic period, a hydrothermal ore-forming period and a hypergenic period. The hydrothermal metallogenic period can be divided into three ore-forming

Table 1 Features of fluid inclusions in calcite in the Huize Zn-Pb- (Ag-Ge) district

Sample No.	Fluid inclusion type	Content of inclusion (%)	Gas-liquid ratio (%)	Size (μm)	Phase state constitution	Testing number (N)	Form of inclusion	Locations
1571-2	Pure liquidus inclusion	40	0	3–5	L	15	Negative crystal, oval, round, liquid dropping and irregular forms	Level 1571 in Qilinchang
	Liquidus inclusion	60	5–10	3–8	L+V			
HQ-84	Pure liquidus inclusion	30	0	3–8	L	12	Oval, liquid dropping, irregular forms with a small number of negative crystal forms.	
	Liquidus inclusion	70	5–20	3–10	L+V			
44-1	Pure liquidus inclusion	30	0	3–15	L	20	Irregular and drawing wire forms as dominant with a small number as crystal and liquid dropping	
	Liquidus inclusion	70	5–15	5–70	L+V			
1631-1	Pure liquidus inclusion	20	0	3–8	L	20	Liquid dropping, round, oval and irregular forms with a small number of negative crystal forms	Level 1631 in Qilinchang
	Liquidus inclusion	80	5–15	3–10	L+V			
HQ109-4	Pure liquidus inclusion	30	0	3–8	L	15	Negative crystal, round, oval and irregular forms	
	Liquidus inclusion	70	5–15	3–10	L+V			
HQ-99-1	Pure liquidus inclusion	30	0	3–8	L	15	Negative crystal, liquid dropping, oval and irregular forms	
	Liquidus inclusion	70	5–10	3–10	L+V			
MQ914	Pure liquidus inclusion	30	0	3–10	L	20	Negative crystal/oval forms as dominant with a small number as irregular/liquid dropping forms	Level 1751 in Kuangshan-chang
	Liquidus inclusion	70	5–20	3–15	L+V			
MQ912	Pure liquidus inclusion	20	0	3–10	L	20	Negative crystal, irregular, oval and liquid dropping forms	
	Liquidus inclusion	80	5–30	3–12	L+V			
YCP-1	Pure liquidus inclusion	30–70	0	3–35	L		Negative crystal, oval, irregular, drawing wire and liquid dropping forms	Yinchangpo
	Liquidus inclusion	70–30	5–20	3–35	L+V			

Analytical unit: Department of Geological Sciences, Kunming University of Science and Technology, Kunming, China. Note: Given for Yinchangpo by Hu (1999) is the average value of 7 samples.

stages: (i) a coarse-grain pyrite-marmatite stage; (ii) a sphalerite-galena stage; (iii) a fine-grain pyrite-calcite stage. Calcite, which is coarse-crystalline granular, rhombic massive and veinlet, is the most important gangue mineral, and is formed at each stage of the hydrothermal metallogenic period. Pyrite is distributed mainly in the orebodies and in the mineralized dolomite of the Baizuo Formation as well as in the NW-extending fault belt; it is distributed as veinlets in galena.

3 Samples and Method

Calcite samples were collected from orebody No.6 of levels 1631 m and 1571 m in the Qilinchang deposit and orebody No.1 of level 1751 m in the Kuangshanchang deposit. After grinding into double-side polished thin slices, the feature of fluid inclusion in calcite was observed under the microscope.

The homogeneous temperature and salinity have been determined in both the heating and cooling stages. A homogenization method was taken to determine the homogeneous temperature of liquid inclusions and a refrigeration method used to determine the salinity. The water constant volume curve (Potter et al., 1978; Zhang and Chen, 1993) and the different-density NaCl constant volume curve of Roedder and Bodnar (1980) were used to estimate the ore-forming pressure.

Sphalerite, pyrite and calcite samples for the composition of fluid inclusions and hydrogen, oxygen and carbon isotope composition were manually washed and selected under a binocular microscope for purity. After that,

samples were poured into a beaker filled with extra pure water, which was then washed for 2–3 h in a supersonic container. Fresh water was poured in 3–5 times onto the pure water in the beaker until the water was very clean. Then the sample-filled beaker was heated with a battery to 80–100°C and made ready for analysis after the moisture had evaporated. The samples of dolomite for oxygen and carbon isotope compositions were ground as fine as –200 mesh under a contamination-free environment. The specimens were prepared at the Super-pure Lab. of the Research Department of Geological Fluids, Institute of Geochemistry, Guizhou. The isotope composition of samples was analyzed at the Isotope Lab. of the Yichang Institute of Geology and Mineral Resources, Ministry of Land and Resources, China.

4 Results

4.1 Features of fluid inclusions

Fluid inclusions in calcite are disposed in a large amount and compactly spread in a group along the calcite crystal plane. According to the distribution state, they all belong to a primary fluid inclusion, but the inclusions are small, most of them 1–10 μm in size. Based on the phase composition and physical states, as well as the study of the nature and mineral inclusions of the Yinchangpo deposit (Hu, 1999), mainly developed in the Huize mine district, there are two sorts of inclusions (Table 1):

Pure liquid inclusion: what is found within the cavity of the inclusions is all single-phase brine liquidus (L) and no vapor phase (V) exists. The fluid inclusions of minerals in

Table 2   Homogeneous temperature and salinity of fluid inclusions of minerals (calcite) in the Huize Zn-Pb- (Ag-Ge) district

Sample No.	Deposit	Ice-melting temperature (°C)	Homogeneous temperature (°C)		Salinity ((wt %NaCl)$_{eq}$)		Pressure (10^{5}Pa)
			Range	Average	Range	Average	
1571-2	Qilinchang	−5.8	168–232	172	7.6–10.8	9.0	543
HQ-84		−4.8	189–240	208	6.3–9.0	7.6	572
631-1		−4.4	142–205	164	5.5–8.5	7.0	463
HQ109-4		−5.7	203–245	221	5.7–10.5	8.8	618
HQ-99-1		−4.1	181–204	193	5.0–7.8	6.6	540
44QM-1		−6.3	147–202	165	8–10.7	9.6	459
MQ914	Kuangshanchang	−7.4	138–226	175	9.4–13.5	11	556
MQ912		−8.2	198–240	217	6.8–16.0	12	661
YCP-1	Yinchangpo	−3.5	98–296	170	1.8–12.5	5.6	410–621

Analytical unit: Department of Geological Sciences, Kunming University of Science and Technology, Kunming, China.
The testing equipments were T1350 heating stages, TRL-02 heating and cooling stages and KBL-1 cooling stages.
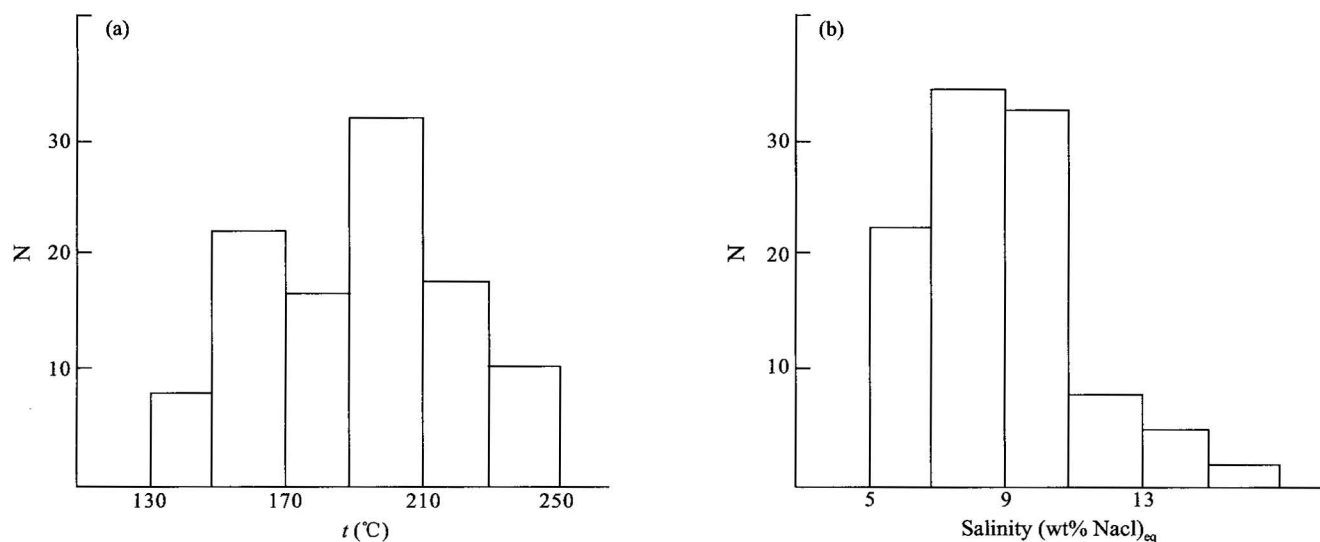Note: Data (7 samples) of YCP-1 are from Hu (1999).

Fig. 2. Diagram of homogeneous temperature-frequency (A) and salinity-frequency (B) in the Huize Zn-Pb-(Ag-Ge) district.

the Qilinchang and the Kuangshanchang deposits are relatively small, mostly around 6–10 μm, while the inclusions of the Yinchangpo deposit are relatively large, mostly around 3–20μm in size and partly around 25–40 μm in size. The morphology of inclusions mostly presents negative crystal form, liquid dropping form, oval form or round form and a small amount of them has irregular forms spread in a group along the calcite crystal plane. The quantity of pure liquid inclusions may take up 30%–40% of the total of the two sorts of inclusion.

Liquid inclusions: the composition of the phase states consists of liquid (L) and vapor phases (V), in a ratio of gas-liquid of 5%–20%. The gas phase often presents in red or black and fiercely pulsates. The morphology of the inclusions is dominated by a negative crystal form and a liquid dropping form, with small amounts in oval, round, or irregular forms. The fluid inclusions of the Qilinchang and

the Kuangshanchang deposits are usually around 3–10 μm in size, while the inclusions of Yinchangpo are relatively large, mostly around 3–20 μm and partly around 25–55μm in size. The quantity of such inclusions may take up 60%–70% of the total of the two sorts of inclusion.

4.2 Homogeneous temperature and salinity of fluid inclusions

In an overall view, the average homogeneous temperature in the calcite fluid inclusion is between 164–221°C and the average salinity is between 5–10.8 wt% (NaCl)$_{eq}$. According to the study by Liu (1996), the average homogeneous temperature observed in the fluid inclusions in deposits is 150–320°C (Table 2, Fig. 2). The decrepitating temperature of pyrite, galena and sphalerite is 140–480°C (Liu and Lin, 1999). As presented, the temperature of ore-forming fluid varies by a wide range,

Table 3 Composition of mineral fluid inclusions of the Huize Zn-Pb-(Ag-Ge) district

Sample No.	Mineral	Gas phase Composition ($\times10^{-6}$)				Liquid phase Composition ($\times10^{-6}$)									Typical value			Locality
		H_2O	CO_2	CO	CH_4	K^+	Na^+	Ca^{2+}	Mg^{2+}	Li^+	F^-	Cl^-	SO_4^{2-}	HCO_3^-	Cl^-/F^-	Na^+/K^+	pH	
HQ99-1	Calcite	320.10	220.56	1.05	0.50	0.53	3.56	108.80	4.16	0.01	0.33	6.01		17.0	18.21	6.72	7.1	Qilinchang
HQ109-4	Calcite	385.55	189.71	1.50	1.01	1.31	7.21	81.50	4.39	0.03	0.42	11.73		141.0	27.93	5.50	7.0	
HQ-84	Calcite	388.61	192.80	1.50	1.05	1.23	7.14	81.44	4.70	0.01	0.41	11.85		141.0	28.90	5.80	7.1	
1631-38	Calcite	402.15	233.65	1.65	1.50	2.45	11.42	72.65	5.56	0.04	0.48	14.90		121.0	31.04	4.66	7.0	
1571-2	Calcite	397.74	211.37	1.50	0.88	1.57	9.30	74.52	4.70	0.02	0.45	12.86		126.0	28.58	5.92	7.1	
1631-7	Sphalerite	310.25	11.40	0.11	0.20	0.81	0.89	26.80	2.06	0.01	0.22	2.50	85.0		11.36	1.10	5.6	
28-2	Sphalerite	310.00	10.50	0.02	0.05	0.28	1.50	0.60	0.01	0.01	0.10	2.60	50.7		26.00	5.36	6.2	
28-3	Sphalerite	375.00	21.80	0.05	0.25	0.75	4.27	6.32	0.73	0.04	0.35	6.88	83.2		19.66	5.69	6.0	
1571-9-9	Pyrite	350.00	11.00	0.02	0.06	0.87	0.25	0.65	0.25	0.02	0.20	1.00	40.5		5.00	0.29	5.6	
MQ-911	Pyrite	440.50	78.20	0.09	0.50	1.81	3.66	51.74	8.15	0.04	0.41	5.21	110.5		12.71	2.02	6.1	Kuangshan-chang
MQ-915	Pyrite	380.00	14.10	0.05	0.35	0.73	3.07	1.39	0.51	0.03	0.25	5.00	78.3		20.00	4.21	5.8	

Notes: Isotope Laboratory of the Yichang Institute of Geology and Mineral Resources, Ministry of Land and Resources by thermal decrepitating-ultrasonic abstraction method.
Testing methods and equipments: Contents of K^+, Na^+, Ca^{2+}, Mg^{2+} and Li^+ were tested by atomic absorption spectrograph (Hitch 180-80 AAS); Contents of Li^+, Cl^- and SO_4^{2-} by the luminosity analytical method (Hitachi 220 Aultraviolet and visible light luminosity); gas phase composition by gas chromatograph (SP-3420 gas chromatograph).

but worthy of note is that the salinity change of some minerals is of a comparatively wide range, which represents different ore-forming stages. However, the salinity is of medium strength, with an average value of 8.5 wt%(NaCl)$_{eq}$. For the sample HQ-99-1, the average homogeneous temperature in the liquid inclusion of calcite is 181–204°C, the average is 193°C. If heated to 245°C, more inclusions are decrepitated and the salinity is 5–7.8 wt%(NaCl)$_{eq}$ with an average of about 6.6 wt%(NaCl)$_{eq}$. Therefore, the ore-forming fluid is of medium temperature and salinity.

4.3 Estimation of ore-forming pressure

The types of fluid inclusion are simple and thus a CO_2-bearing type liquid inclusion is not seen. Therefore, the same homogeneous temperature and salinity of liquid inclusions can be adopted to obtain fluid density. From this the pressure relationship for low-medium salinity inclusions can be used to estimate the ore-forming pressure. The pressure value shown in Table 2 is a saturated vapor pressure, but it does not represent ore-forming pressure. In fact, it is only an approximate value (410×10^5–661×10^5 Pa) of the ore-forming pressure (Table 2).

4.4 Feature of Fluid Inclusion Compositions

The main composition of the gas phase in various fluid inclusions (Table 2) is H_2O, CO_2, CO, CH_4 and H_2 with H_2

as a minimum; the main liquid phase composition is K^+, Na^+, Ca^{2+}, Mg^{2+}, F^-, Cl^-, SO_4^{2-}. Generally speaking, Na^+, Cl^-, Ca^{2+}, Mg^{2+}, F^- and K^+ with $Na^+>K^+$, $Cl^->F^-$, $Ca^{2+}>Mg^{2+}$ are enriched in calcite and metallic minerals, which forms the basic feature of the ore-forming fluid. According to the study by Liu (1996), the mineral fluid inclusion of the deposits contain Pb, Zn, so the property of the ore-forming fluid is of Na^+–K^+–Ca^{2+}–Cl^-–F^-–SO_4^{2-} containing Pb and Zn.

5 Discussion

5.1 Relationship of various ions

It can be seen from Fig. 3 that the contents of Na^+–K^+, Cl^-–F^- and the ratios of Na^+/K^+–Cl^-/F^- show a good linear relationship. The tested calcite is formed in the later ore-forming stage, while galena and tested pyrite are formed in the main ore-forming stage. In calcite the ratios of Na^+/K^+ and Cl^-/F^- are relatively higher, while in sphalerite and pyrite the ratios of Na^+/K^+ and Cl^-/F^- are relatively high and Na^+/K^+ ratio increases in parallel with Cl^-/F^- ratio, which reflects that from the later ore-forming to the earlier ore-forming stages; the contents of K^+ and F^- in the ore-forming fluids tends to increase. The enrichment of K^+ and F^- is an indicator component of deep source in relationship with magmatic hydrothermalism, so, it can be concluded that there is a deep source component to the initial ore-

Table 4   Carbon, hydrogen and oxygen isotopic composition of minerals and rocks in the Baizuo Formation in the Huize deposits

Sample No.	Mineral or rock	T_0 (°C)	$\delta^{13}C$ V-PDB (‰)	$\delta^{18}O$ V-SMOW (‰)	$\delta^{18}O$ V-PDB (‰)	$\delta^{18}O$ (‰) (fluid)	δD (‰)	Locality	Ref.
HQO-99-1	Calcite	193	−1.94	17.088	−13.36	7.78	−43.5	Orebody No. 6 at level 1631 in the Qilinchang deposit	
HQO-109-4	Calcite	221	−3.27	17.789	−12.68	10.08	−54.8		
1631-38	Calcite	164	−2.97	18.562	−11.93	7.78	−48		1
HQ-84	Calcite	208	−3.23	18.211	−12.27	9.7	−51.5	Orebody No. 6 at level 1571 in the Qilinchang deposit	
HQ-109-4	Calcite	221	−3.31	17.789	−12.68	7.55	−43.5		
1571-2	Calcite	172	−3.3	18.211	−12.27	7.7	−55.4		
Hui-2-3	Calcite	180	−2.75	17.8	−12.67	7.14		Orebody No. 6 at level 1751 in the Qilinchang deposit	
38-3	Calcite		−2.8	17.1	−13.4	6.44		Orebody No. 6 at level 1884 in the Qilinchang deposit	
Hui-6-10	Calcite		−2.9	17.8	−12.6	7.14		Orebody No. 6 at level 1648 in the Qilinchang deposit	
13-61	Calcite		−2.7	18.1	−12.4	7.44		Orebody No. 6 at level 1691 in the Qilinchang deposit	
Hui-1-1	Calcite		−3.2	18.43	−12.06	7.77		Orebody No. 6 at level 1836 in the Qilinchang deposit	2
14-2-8	Calcite		−2.6	18.7	−11.8	8.04		Orebody No. 6 at level 1631 in the Qilinchang deposit	
14-3-6	Calcite		−2.7	18.4	−12.1	7.74			
Hui-1-2	Near-ore dolomite		0.77	21.16	−9.41				
Hui-5-1	Calcite		−2.4	18.1	−12.3	7.44		Orebody No. 6 at level 1571 in the Qilinchang deposit	
Hui-4-23	Calcite		−3.1	17.5	−13	6.84			
23-4R	Calcite		−3	17.6	−12.8	6.94			
HQC-25	Barite-bearing Pb-Zn mineralized broken dolomite		0.3	20.4	−10.1			Orebody No. 6 at level 1631 in the Qilinchang deposit	1
HQC-98	Pb-Zn mineralized dolomitic cataclasite		−3.2	19.5	−11				
HQC-92	Pb-Zn mineralized dolomitic cataclasite		−1.6	17.8	−12.7				
14-3-19	Near-ore altered dolomite		−0.8	20.5	−10.1				3
Hui-8	Barite	140		8.29			−2.05	Kuangshanchang deposit	2
HE16	Bioclastic irregular limestone		−0.44	22.45	−8.16			At level 2233 in the Kuangshanchang deposit	4
HE18	Bioclastic irregular limestone		−1.5	21.33	−9.24				
HE17	Fine-medium-crystalline dolomite		0.85	20.98	−9.58				
SC-33	Dolomitic limestone		−0.9	21	−9.6			Sunjiagou section in the periphery of the district	1
SC-34	Coarse-crystalline dolomite		−2.2	20.5	−10.1				
SC-35	Coarse-crystalline dolomite		−1.2	21.4	−9.2				
HE11	Fine-medium-crystalline dolomite		0.85	19.32	−11.19			Zhujiayakou in the periphery of the district	
HE10	Shell-bearing dolomitized limestone		−3.35	19.42	−11.1				
HE12	Shell-bearing dolomitized limestone		−1.1	20.09	−10.45				4
HE02	Fine-medium-crystalline dolomite		0.09	22.6	−8.01			Qingchaojie in the periphery of the district	
HE01	Bioclastic irregular limestone		−1.15	22.59	−8.02				
HE03	Dolomitized limestone		−0.53	23.14	−7.49				

Notes: $\delta^{13}C$ V-PDB was tested by the Center of Geological Analysis and Research, Ministry of Nuclear Industry, and equipment type is MAT252. The analytical unit of $\delta^{18}O$ and δD was the Yichang Institute of Geology and Mineral Resources, Ministry of Land and Resources. Analytical method of $\delta^{18}O$ was 100% phosphorus acid. Type of mass spectrometer: MAT 251 EM, analytic precision: ±0.2%. Analytical method of δD was BrF5, type of mass spectrometer: MAT 251 EM, analytic precision: ±0.2%. $\delta^{18}O_{H_2O}$ was calculated on the basis of $1000\ln\alpha_{\text{calcite-fluid}} = 2.78 \times 10^6 T^{-2} - 2.89$ (O'Neil et al., 1969). The numerals in parentheses stand for the measured values of coexisting metallic sulfides. References: 1. this work; 2. Liu and Lin (1999); 3. Zhou (1996); 4. Chen (1984).
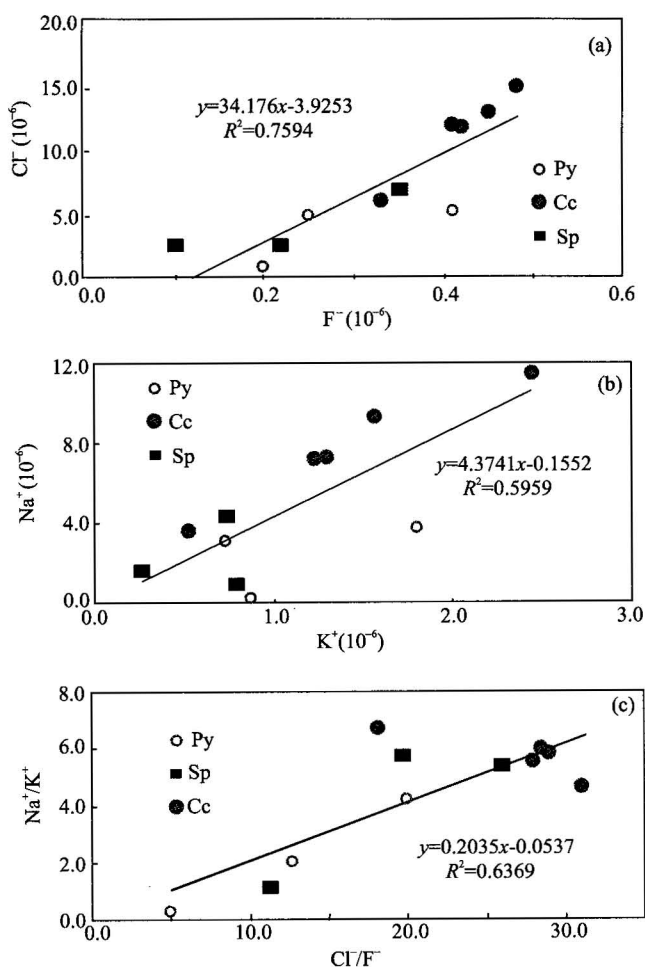
Fig. 3. Interrelationship of different compositions in the ore-forming fluid of the Huize Zn-Pb-(Ag-Ge) district.

A, Cl^--F^-; B, Na^+-K^+; C, Na^+/K^+-Cl^-/F^-; Py – pyrite; Cc – calcite; Sp – sphalerite.

forming fluid.

5.2 Carbon, hydrogen and oxygen isotopic compositions

The C, H and O isotopic compositions of gangue calcite represent that of the metallogenic fluids. Taking into account the geological conditions of deposits, it is deduced that the ore-forming fluids were mainly derived from metallogenic material-rich metamorphic water and magmatic water. In fact, this results in a mixing metallogenic hydrothermalism (Fig. 4).

The carbon and oxygen isotopic composition of calcite ($\delta^{13}C_{V-PDB}$: $-1.94\%o$ to $-3.31\%o$, $\delta^{18}O_{V-SMOW}$: $17.09\%o$–$18.56\%o$) is different from that of the ore-hosting dolomite ($\delta^{13}C_{V-PDB}$: $-3.35\%o$ to $0.85\%o$, $\delta^{18}O_{V-SMOW}$: $17.80\%o$ to $23.14\%o$), and also from that of the deep source ($\delta^{13}C_{V-PDB}$: $-4\%o$ to $-10\%o$) (Zhang, 1995). From unaltered dolomite via altered dolomite to calcite either from the Qilinchang

deposit or from the Yinchangpo deposit, their C and O isotopic composition displays obvious linearity, with $\delta^{13}C$ and $\delta^{18}O$ values tending to decrease progressively toward the deep source. Therefore, it can be supposed that the initial metallogenic fluid was derived from a deep source and carbon in the calcite is the mixture of crust-source carbon in the rocks of the strata and deep-source carbon.

5.3 Strontium isotopic composition

The $^{87}Sr/^{86}Sr$ values of sulfide ores from the Qilingchang Zn-Pb-(Ag-Ge) deposit are within the range of 0.71021–0.71768, and the initial ratio of $^{87}Sr/^{86}Sr$ is 0.7114 (7 samples). The $^{87}Sr/^{86}Sr$ values of sulfides and gangue minerals from the Qilingchang deposit are within the range of 0.70832–0.71808 (Zhou et al., 2001). In his research of the Yinchangpo deposit, Hu (1999) reported that the Baizuo Formation dolomite, gangue mineral (calcite) and ore show differences in $^{87}Sr/^{86}Sr$ ratios. The minimum of $^{87}Sr/^{86}Sr$ value for the dolomite (0.70868–0.7093) is close to the initial $^{87}Sr/^{86}Sr$ ratio of the contemporaneous Carboniferous seawater (0.708–0.709); the initial $^{87}Sr/^{86}Sr$ ratio of sulfide ore is 0.71084–0.71877 and those of calcite are 0.72227–0.72557. The $^{87}Sr/^{86}Sr$ ratio of sulfides and calcite from the deposits should represent those at the time of interaction between ore-forming fluid and the wall rocks during the metallogenic period, and they are obviously higher than those of the wall rocks and contemporaneous seawater, implying that the original metallogenic fluid flowed through a radiogenic Sr-source region.

From the viewpoint of the regional geological conditions, the basement Kunyang Group in this region exhibits high $^{87}Sr/^{86}Sr$ values. The Yingmin Formation dolomite of the Kunyang Group from the Yimen copper deposit has a $^{87}Sr/^{86}Sr$ ratio of 0.7281 (Ran and Liu, 1993), indicating strontium pertaining to radioactive strontium. The metallogenic fluid reacted with carbonate (water/rock interaction) in the strata during its ascension, thus leading to significant differences in strontium isotopic composition for the wall rock, ore and calcite. Based on the Sr isotopic composition of galena ($^{87}Sr/^{86}Sr$ ratio from 0.71092 to 0.71451) and sphalerite ($^{87}Sr/^{86}Sr$ ratio from 0.70808 to 0.71490), that from the Qilinchang deposit is lower than that of the regional rocks. Zhou et al. (2001) considered that the strontium would be impossible to have derived from the ore-hosting wall-rock. It is therefore deduced that the strontium in the Huize Zn-Pb-(Ag-Ge) deposits is a mixture of strontium derived from different source regions in the Kunyang Group basement rocks and/or even deep magmatic hot fluid.

With a systematic study of the geochemistry of rare earth elements of calcite, Huang et al. (2001) thought that the
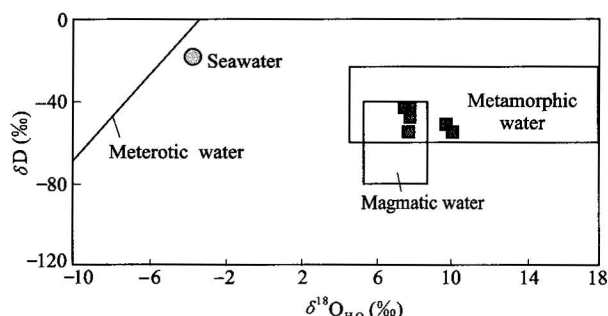
Fig. 4. $\delta^{18}O_{H_2O}$-δD plot in the Huize Zn-Pb-(Ag-Ge) district.

ore-forming fluid has features of multiple sourcing and the mantle fluid motion plays an important role in the process of ore-forming fluid formation, which supports the deduction of deep source ore-forming fluid.

6 Conclusion

The ore-forming fluid in the Huize Zn-Pb-(Ag-Ge) deposits exhibits medium-high temperature, medium salinity and pressure, and the hydrothermal fluid is of Na^+-K^+-Ca^{2+}-Cl^--F^--SO_4^{2-} type containing rich Pb and Zn. Compared with the MVT-type Pb-Zn deposit (Kyle, 1981; Rhodes and Lantos, 1984; Sverjensky, 1986; Bethke and Marshak, 1990; Brannon et al., 1992; Ge and Garven, 1992; Garven et al., 1993; Garven, 1994; Titley, 1993, 1996; Eisenlohr et al., 1994; Christensen et al., 1995a, b), there is a large difference in salinity, ore-forming temperature, trace element, etc. (Han et al., 2002).

Based on the above discussion, a conclusion can be drawn that the ore-forming fluids in the Huize Zn-Pb-(Ag-Ge) deposits might be derived from metallogenic material-rich metamorphic water and magmatic water, in view of their relation to the metamorphism of the Kunyang Group in the basement and the magmatic hot fluid. The deposit might have resulted from a cyclically ascending ore-forming fluid rich in Pb, Zn from depth that penetrated along the ore-hosting structure.

Acknowledgements

References

Bethke, C. M., and Marshak, S., 1990. Brine migrations across North America—the plate tectonics of ground water. *Ann. Rev. Earth Planet. Sci.*, 18: 287–315.

Bierlein, F. P., Ashley, P. M., and Seccombe, P. K., 1996. Origin of hydrothermal Cu-Zn-Pb mineralization in Olary Block, south Australia: evidence from fluid inclusions and sulfur isotopes. *Precambrian Res.*, 79 (3–4): 281–305.

Brannon, J. C., Podosek, F. A., and McLinmans, R. K., 1992. Alleghenian age of the Upper Mississippi Valley-type zinc-lead deposit determined by Rb-Sr dating of sphalerite. *Nature*, 356: 509–511.

Chen Jin, 1993. Probe on formation of Pb-Zn sulphide ore and ore-forming model of the Qilinchang deposit. *Nonferrous Metallic Mineral and Exploration*, (2): 85–90 (in Chinese with English abstract).

Chen Shijie, 1984. A discussion on the sedimentary origin of Pb-Zn deposits in western Guizhou and northeastern Yunnan. *J. Guizhou Geol.*, 8(3): 35–39 (in Chinese with English abstract).

Christensen, J.N., Halliday, A.N., Leigh, K.E., Randell, R.N., and Kesler, S.E., 1995a. Direct dating of sulfides by Rb-Sr: a critical test using the Polaris Mississippi Valley-type Zn-Pb deposit. *Geochem. Cosmochem. Acta*, 59: 5191–5197.

Christensen, J.N., Halliday, A. N., Vearncomble, J. R., and Kesler, S. E., 1995b. Testing models of scale crustal fluid flow using direct dating of sulfides: Rb-Sr evidence for early dewatering and formation of Mississippi Valley-type deposits, Canning Basin, Australia. *Econ. Geol.*, 90: 877–884.

Eisenlohr, B.N., Tompkins, L.A., Cathies, L.M., Bariey, M.E., and Groves, D.L., 1994. Mississippi Valley-type Zn-Pb deposits: products of brine expulsion by eustatatically induced hydrocarbon generation: an example from northwestern Australia. *Geology*, 22: 315–318.

Ettner, D. C., Bjorlykke, A., and Andersen, T., 1993. Fluid evolution and Au-Cu genesis along a shear zone; a regional fluid inclusion study of shear zone-hosted alteration and gold and copper mineralization in the Kautokeino greenstone belt, Finnmark, Norway. *J. Geochem. Explor.*, 49: 233–267.

Fyfe, W.S., Price, N. J., and Thompson, A. B., 1978. *Fluid in the Crust*. New York: Elsevier, 383.

Ge, S., and Garven, G., 1992. Hydromechanical modeling of tectonically driven groundwater flow with application to the Arkoma foreland basin. *J. Geophys. Res.*, 97(B6): 9119–9144.

Garven, G.., Ge, S., Person, M. A., and Sverjensky, D. A., 1993. Genesis of stratabound ore deposits in the Midcontinent basins of North America. 1–The role of regional groundwater flow. *Am. J. Sci.*, 293: 497–568.

Garven G., 1994. Genesis of stratabound ore deposits in the Midcontinent basins of North America. 1–The role of regional groundwater flow, a reply. *Am. J. Sci.*, 294: 760–775.

Han Runsheng, Liu Congqiang, Huang Zhilong, Ma Deyun and Li Yuan, 2000. Features of structural control of minerals and fault

structural rock rare earth element for Huize Pb-Zn Deposit, Yunnan. *J. Mineral. Petrol.*, 20(4): 11–18 (in Chinese with English abstract).

Han Runsheng, Chen Jin, Li Yuan, Ma Deyun, Zhao Deshun and Ma Gengsheng, 2001a. Law of structural control of mineralsand prediction of concealed ore for the Huize Pb-Zn deposit, Yunnan. *Acta Mineral. Sinica*, 21 (2): 265–269 (in Chinese with English abstract).

Han Runsheng, Liu Congqiang, Huang Zhilong, Chen Jin, Ma Deyun and Li Yuan, 2001b. Ore-forming model of Huize rich Pb-Zn deposit, Yunnan. *Acta Mineral. Sinica*, 21(4): 674–680 (in Chinese with English abstract).

Han Runsheng, Liu Congqoang, Huang Zhilong, Ma Deyun, Chen Jin, Lei Li and Yang Hailin, 2002. Huize Carbonate-hosted rich Zn-Pb- (Ag) District, Yunnan, China. *Ore Geology Reviews* (in press).

Hu Yaoguo, 1999. Preserving State, Source of ore-forming substances and ore-forming mechanism of rich Ag metallic deposit in Yinchangpo, Guizhou. *Unpublished doctoral science thesis*. Geochemistry Research Institute of the Chinese Academy of Sciences, 65–67 (In Chinese with English abstract).

Huang Zhilong, Chen Jin, Han Runsheng, Li Wenbo, Gao Derong, Zhao Deshun and Liu Congqiang, 2001. REE geochemistry of mineral calcite in Yunnan Huize Pb-Zn deposit. *Acta Mineral. Sinica*, 21(4): 659–666 (in Chinese with English abstract).

Jia Yaoming, 1996. Study on fluid ore-forming system and function. *Earth Sci. Frontier*, 3(3–4): 253–258 (in Chinese with English abstract).

Kyle, R. J., 1981. Geology of the Pine Point lead-zinc district. In: Wolf, K. H., (ed.), *Handbook of strata-bound and stratiform ore deposits*. New York: Elsevier, 9: 643–741.

Li Zhaolin, Yang Rongyong and Sun Xiaoming, 1996. Fluid formation, evolution and ore-formation in geological function. *Earth Sci. Frontier*, 3(3–4): 237–244 (in Chinese with English abstract).

Liao Wen, 1984. Discussion on feature of S-Pb isotope composition and ore-forming mode in Pb-Zn metallic zone in east Yunnan and west Guizhou. *Geology and Prospecting*, (1): 1–6 (in Chinese with English abstract).

Liu Hechang and Lin Wenda, 1999. *Study on Pb-Zn-Ag Ore Deposit Law in Northeast Yunnan*. Kunming: Yunnan University Press, 250–496 (in Chinese).

Liu Hechang, 1996. Ore-forming model in Pb-Zn ore-forming zone in Yunnan, Sichuan and Guizhou, *Yunnan Geol.*, 15(1): 41–51 (in Chinese with English abstract).

Lu Huanzhang, 1997. *Ore-forming Fluid*. Beijing: Science and Technology Publishing House, 2–98 (in Chinese with English abstract).

Lu Huanzhang, 1998. Working Method for studying fluid in the crust. *Earth Sci. Frontier*, 5(1–2): 295–300 (in Chinese with English abstract).

Mao Jingwen and Li Yinqing, 2001. Study on fluid inclusion of telluride gold deposit in Dongping, Hebei: Relationship between the mantle fluid and ore-formation. *Ore Deposit Geology*, 20(1): 23–36 (in Chinese with English abstract).

Mao Jingwen, Hua Renming and Li Xiaobo, 1999. Discussion on large-scale ore-forming function and large-sized ore assemblage zone. *Ore Deposits*, 18(4): 291–299 (in Chinese with English abstract).

Meissner, K., and Wever, R., 1992. Possible role of fluid for structuring continental crust. *Earth Sci. Rev.*, 32: 19–32.

O'Neil, J. R., Clayton, R. N., and Mayada, T. K., 1969. Oxygen isotope fractionation in divalent metal carbonates. *J. Chem.*

Phys., 51: 5547–5558.

Parry, W.T., 1998. Fault-fluid compositions from fluid-inclusion observations and solubility of fracture-sealing minerals. *Precambrian Res.*, 290 (1–2): 1–26.

Peng Jiantang and Dai Tagen, 1999. Study on geochemistry of ore-forming fluid of gold deposit in southwest Hunan. *Ore Deposits*, 18 (1): 73–82 (in Chinese with English abstract).

Polliand, M., and Moritz, R., 1999. Basement-hosted quartz-barite sulfide veins in the French Alps: a record of Alpine tectonic fluid expulsion in external crystalline massifs—structural, fluid inclusion, and isotopes (S and Sr) evidence. *Econ. Geol.*, 94: 37–56.

Potter, R. W., Clynne, M.A., and Brown D.L., 1978. Freezing point deposition of aqueous solution chloride solutions, *Econ. Geol.*, 73: 284–285.

Ran Congying and Liu Weihua, 1993. *Geochemistry of Copper Deposits in the Kangdian Axis and the Mechanism of Their Ladder-pattern Texture*. Beijing: Science Press, 141–148 (in Chinese with English abstract).

Rhodes, D., and Lantos E.A., 1984. Pine Point ore bodies and their relationship to the stratigraphy, structure, dolomitization, and karstification of the middle Devonian barrier complex. *Econ. Geol.*, 79: 8.

Robert, F., Boullier, A. M., and Firdaous, K., 1995. Gold-quartz veins in metamorphic terranes and their bearing on the role of fluids in faulting. *J. Geophys. Res.*, 100 (B7): 12861–12879.

Roedder, E., and Bodnar, R. J., 1980. Geologic pressure determinations from fluid inclusion studies. *Ann. Rev. Earth Planet. Sci.*, 8: 263–301.

Sverjensky, D. A., 1986. Genesis of Mississippi Valley-type lead-zinc deposits. *Ann. Rev. Earth Planet. Sci.*, 14: 177–179.

Titley, S. R., 1993. Characteristics of high temperature carbonate-hosted massive sulfide ores in the United States, Mexico and Peru. In: Kirkham R. V., Sinclair, W. D., Thorpe, R. I., and Duke, J. M. (eds.), *Mineral Deposit Modeling*. Geol. Assoc. Can. Spec., 585–614.

Titley, S. R., 1996. Characteristics of high temperature, carbonate-hosted replacement ores and some comparisons with Mississippi Valley-type ores. *Society of Economic Geologists Special Publication*, (4): 244–254.

Zhai Yusheng, 1996. Some questions on structural fluid-ore-forming study. *Earth Sci. Frontier*, 3(4): 230–236 (in Chinese with English abstract).

Zhang Ligang, 1995. *Application of Stable Isotope in Geological Science*. Xi'an: Shaanxi Science and Technology Publishing House, 65 (in Chinese).

Zhang Weiji, 1984. Discussion on sedimentary formation and ore-forming law of Pb-Zn deposit in northeast Yunnan. *Geology and Prospecting*, (7): 11–16 (in Chinese with English abstract).

Zhang Wenhuai and Chen Ziying, 1993. *Geology of fluid inclusion*. Wuhan: China Geology University Press, 154–155, 138–139 (in Chinese with English abstract).

Zhao Zhun, 1995. Ore-forming model of Pb-Zn deposit in east and northeast Yunnan. *Yunnan Geol.*, 14 (4): 350–354 (in Chinese with English abstract).

Zhou Chaoxian, 1996. *Origin of Mineralizing Metals, Geochemical Characteristics of Ore-forming Fluid and Genesis of the Qilinchang Zn-Pb Deposit, Northeast Yunnan Province, China*. Unpublished Master of Science thesis, Guiyang, Institute of Geochemistry, Chinese Academy of Sciences, 84 (in Chinese with English abstract).

Zhou, C., Wei, C., Guo, J., and Li, C., 2001. The source of metals in the Qilinchang Pb-Zn deposit, Northeastern Yunnan, China: Pb-Sr isotope constraints. *Econ. Geol.*, 96: 583–598.